Abstract submitted to the 53st AIAA Aerospace Sciences Meeting
To be held at Kissimmee, Florida, January 5-9, 2015

(Technical Topic: Meshing, Visualization, and Computational Environments)

Visualization and Quantification of Rotor Tip Vortices in Helicopter Flows

David L. Kao[1], Jasim U. Ahmad[2], Terry L. Holst[3]
NASA Ames Research Center, Moffett Field, CA

ABSTRACT

This paper presents an automated approach for effective extraction, visualization, and quantification of vortex core radii from the Navier-Stokes simulations of a UH-60A rotor in forward flight. We adopt a scaled Q-criterion to determine vortex regions and then perform vortex core profiling in these regions to calculate vortex core radii. This method provides an efficient way of visualizing and quantifying the blade tip vortices. Moreover, the vortices radii are displayed graphically in a plane.

I. Introduction

Helicopter aerodynamics encompasses a highly vortical flow field. The vortices generated at the blade tip contain very unsteady, complex, three-dimensional structures. They undergo several changes at the rotor wake, particularly their interactions with other blades, fuselage, and various components of the helicopter. It is crucial to investigate the vortex kinematics and their subsequent dynamic evolution. Many researches have been devoted to the understanding of the dynamic evolution of vortices. Most of these are experimental methods [Yamauchi et al. '12, Bhagwat et al. '00, Leishman and Bagai '98], [Bhagwat and Leishman '98], [McAlister & Heineck '02], [Mula et al. '11], [Ramasamy et al. '11], and [Yamauchi et al. '12] and some analytical methods applied to Computational Fluid Dynamics (CFD) data. One important experimental approach is to use the Particle Image Velocimetry (PIV) measurement technique. In a recent study, the characteristics of vortices captured on the PIV plane from the full-scale UH-60A wind tunnel test were compared against CFD calculations [Ahmad et al. '13]. This study provided a comprehensive comparison of the vortex characteristics using the method described in [Yamauchi et al. '12].

In May 2010, PIV measurements of a full-scale UH-60A rotor were acquired in the National Full-Scale Aerodynamics Complex (NFAC) 40- by 80-Foot Wind Tunnel [Yamauchi et. al '12]. The experimental data provided a way of validating high-fidelity CFD and Computational Structural Dynamics (CSD) simulations of vortical helicopter flow fields. The key region of interest was located at the PIV plane, where measurements were acquired. In that experiment, PIV image data was processed to create ensemble averaged velocity and vorticity fields. As for the computational approach, several CFD simulations of the UH-60A rotor using the Navier-Stokes equations were performed based on the same run conditions as that employed in the wind tunnel tests. Furthermore, the numerical studies compared cases where the UH-60A was in free air versus in the wind tunnel with walls were included in the simulation. To model the rotor wakes as accurately as possible, one of the numerical studies also adopted an Adaptive Mesh Refinement (AMR) gridding system.

The present study provides an analysis as well as visualization of blade tip vortices on the PIV plane. Unlike a conventional method, where the user would manually select a vortex core and then trace a line across the vortex center to obtain its cross-flow profile, the new approach proposed in this paper is fully automatic and does not require any user intervention. In addition, it is extended to support CFD solutions resulting from the AMR gridding method. A typical method is to display contours of the cross-flow vorticity on the PIV plane. With a scalar field

---

[1] Researcher, NASA Advanced Supercomputing Division, M/S N258-5.
[2] Aerospace Engineer, NASA Advanced Supercomputing Division, M/S N258-2, Member AIAA.
[3] Branch Chief, Fundamental Modeling and Simulation Branch, NASA Advanced Supercomputing Division, M/S N258-2, AIAA Fellow.

visualized through color mapping, the flow features revealed by contours would vary with the color map levels. For example, the color map of a cutting plane of the vorticity magnitude determines how much of a vortex structure is actually revealed. The vortex core structure may appear larger or smaller, depending on the specific contour levels. Thus, the resulting visualization is sensitive to the (number of) user-specified contour levels. For vortex core radius measurements, it is more accurate to determine the core radius by the profile of the cross-flow velocity across the vortex core. Often, the cross-flow velocity profiling task is time-consuming since the user needs to manually select the core center and then specify sampling points along the velocity profile axis. This process becomes even more compute-intensive when the associated grid system is very large, e.g. with hundreds of millions of grid points. The following section introduces the vortex core radius extraction algorithm as it is applied to CFD solutions.

II. Approach

A. Computational PIV Plane

For appropriate validation of computational results with experimental data, a Cartesian experimental grid plane is created. This Cartesian plane is hereafter referred to as *the PIV plane*. In the experiment [Yamauchi et al. '12], the PIV plane, 3.5 ft. high by 14 ft. wide, is parallel to the YZ plane and is 21.5 inches behind the advancing blade when it is in the 90 deg azimuth position.

The simulation uses multi-zone structured OVERSET grids [Meakin '93]. To determine the intersection of the PIV plane with these grid zones, an iso-surface algorithm is applied to locate the portion of the PIV plane that lies in each grid zone. Fortunately, only a small subset of the off body level 1 (L1) grid zones is needed for the iso-surface extraction. Figures 1A and 1B illustrate how the PIV plane is represented by a set of iso-surfaces for two case studies. In Fig. 1A, the PIV plane spans across two grid zones for a simulation case which is based on an gridding system with 62 zones while in Fig. 1B, the PIV plane spans across many zones for a simulation which is based on an AMR gridding system.

To determine the vortex core radius at a point near the vortex center, it is necessary to obtain the cross-flow velocity along a line that crosses the vortex core. As the iso-surfaces are made up of disjoint triangles, it is difficult to get this data along a line. Instead a uniform grid with a finer resolution that overlays the iso-surfaces is created. This uniform grid represents the computational PIV stated above. For the present study, the grid spacing is set to be the smallest grid spacing used in the AMR grid case. This ensures that the fine detail of the flow data is not missing.
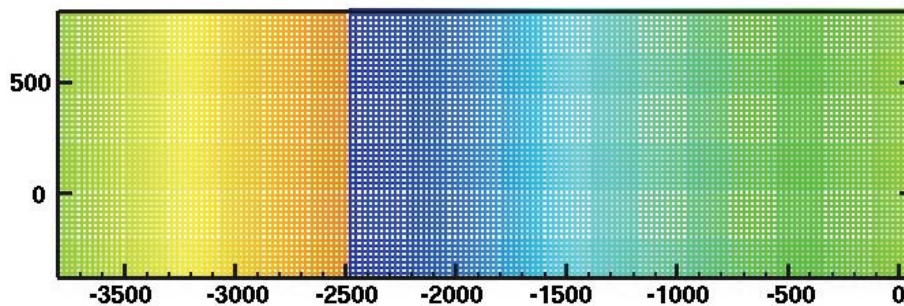

Figure 1A. The PIV plane represented by two iso-surfaces across two grid zones that intersect the PIV plane, with the vertices of the iso-surfaces color-mapped by the vertex index.
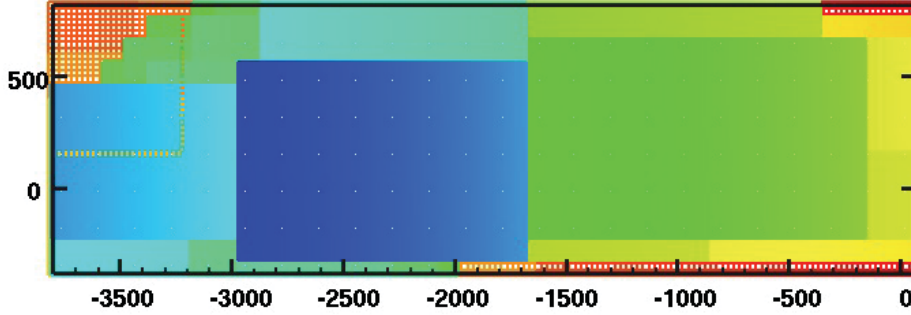
Figure 1B. The PIV plane represented by multiple iso-surfaces in an AMR grid case with the vertices of the iso-surfaces color-mapped by the vertex index.

B. Velocity Interpolation

With the Cartesian plane created, the next step is to interpolate the solution data at all grid points on the plane. Several methods can be used for this task. One simple yet brute force approach is to perform interpolation from the solution data associated with the original multi-zone grids. For each grid point p in the Cartesian plane, search for the grid cell that contains p from all grid cells of the multi-zone grid. However, this could be computationally expensive because one needs to employ a search algorithm. An alternative method is to interpolate data based on the iso-surfaces, which were discussed in Section II.A. For each grid point p in the Cartesian plane, search for the iso-surface triangle that contains p. This is preferred to the brute force approach since it only needs to search for all triangles of the iso-surfaces instead of all grid cells of the multi-zone grid. However, this method can still be compute-intensive if there are thousands of iso-surface triangles. Thus, a new method is proposed in the present study. It is more efficient than the two aforementioned approaches and is based on the observation that the number of grid points in the multi-zone grids is far larger than that of vertices of the iso-surfaces that represent the PIV plane. For example, the gridding system for the UH-60A in the free air case consists of approximately 78 million grid points, whereas the number of vertices of the iso-surfaces is only about 7.5K (in the form of 14K triangles). For the adaptive case, the grid system generates approximately 725 million grid points, whereas the number of vertices of the iso-surfaces is approximately 46K (with 88K triangles) only. The basic idea of our strategy is to locate the grid points (of the Cartesian plane) inside each triangle of the iso-surfaces. Then, the velocity at each such grid point is obtained by interpolating the data across the vertices of the triangle. Once all iso-surface triangles are processed, every grid point on the Cartesian plane will be assigned the interpolated velocity data. Due to the nature of OVERSET grids, a grid point on the Cartesian plane may reside in two or more iso-surface triangles. In this scenario, the velocity at that grid point is determined by the velocity data of the smallest triangle. This situation occurs frequently in solution cases based on AMR grids.

C. Cross-flow Velocity Profiling

With the velocity data interpolated for all grid points on the computational PIV plane, the next step is then to calculate the vortex core radius from the cross-flow velocity components. A typical approach is to first plot a cross-flow velocity profile of a vortex core. Then, the core diameter can be obtained by calculating the distance between the point of local minimum and that of local maximum with regard to the cross-flow velocity magnitude. One challenge with this approach is that the user needs to manually pick a vortex core center and therefore this task can be time consuming. In addition, the user may not know the exact position of the vortex core center. A popular method is to plot a contour map of the vorticity magnitude, by which the vortex core center is then selected. However, it requires user intervention and the vortex core radius can be calculated only at discrete points selected by the user. A second challenge with this approach is that the vortex filament may not be perpendicular to the PIV plane. Thus, a more accurate approach is to plot velocity profile along two orthogonal axes. The final vortex radius is then the average of the core radii calculated from the two cross-flow velocity profiles.

D. Automatic Vortex Core Radius Extraction

3

In the present study, several methods are investigated for calculating the vortex core radius. Given a grid point, the cross-flow velocity profile is computed for two orthogonal axes with the common origin at the grid point. This approach is straightforward, though the core radius color map may not be easy to understand. Figure 2 shows the vortex core radius for the flow solution case with wind tunnel walls, while there are several regions with large vortex core radii in the color map. Figure 3 shows a plot of the vortex core radius at grid points where the vorticity magnitude is above a threshold value. The disadvantage of this approach is that the user needs to specify a threshold. Governed by the threshold, fewer or more grid points may be needed for the vortex core radius calculation.

A more preferable method is to obviate the necessity for the user to specify a threshold while automatically calculating the vortex core radius. The user-specified threshold values can be for any scalar quantity such as vorticity magnitude, $\lambda-2$, or the Q-Criterion. In this present study, we propose to adopt scaled Q-Criterion that is non-dimensional [Kamkar et al. '11]. The advantage of the scaled Q-Criterion is that a threshold value of 1 always refers to the vortex core boundary. By calculating the vortex core radii at grid points where the scaled Q-Criterion is greater than or equal to 1, it automatically produces a vortex core color map that gives a clear delineation of the vortex strength across the PIV plane. Figure 4 shows a color map of the vortex core radius based on the scaled Q-Criterion.

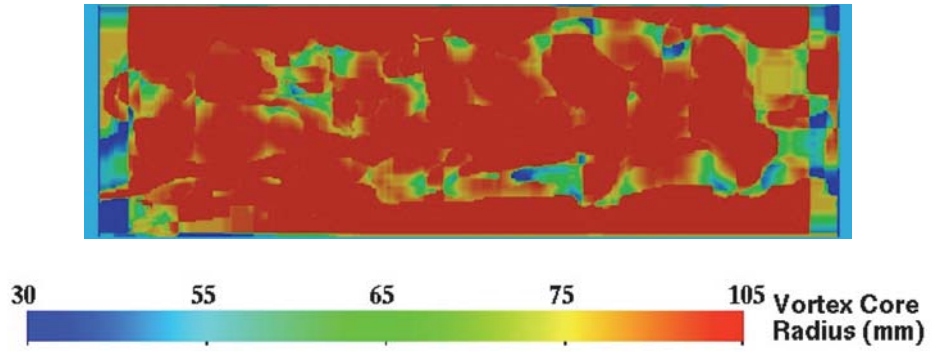American Institute of Aeronautics and Astronautics

Figure 2. A color map of the vortex core radius on the PIV plane. The core radii are calculated for all grid points on the PIV plane.
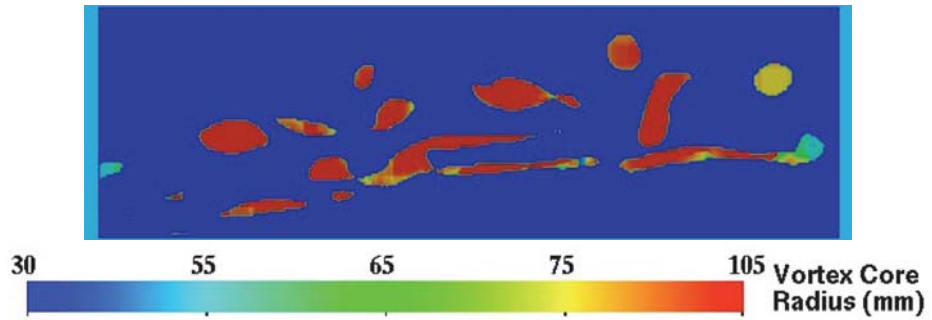

Figure 3. A color map of the vortex core radius. The core radii are calculated for all grid points on the PIV plane with the vorticity magnitude great than 64 1/s.

Figure 4. The vortex core radii at the grid points where the scaled Q-criterion is great than or equal to 1.

III. Results

Our approach described in the previous section has been applied to two simulation studies of a UH-60A rotor [Ahmad et al. '13]. In the final paper, results from additional case studies will be provided and analyzed in more detail. These simulation studies are based on Run 73, i.e., one of the test conditions under which the PIV data were acquired in the aforementioned wind tunnel test. Run 73 is a low-speed free stream flow with significant Blade Vortex Interactions (BVI). Some of the important parameters for this case are: the advance ratio $\mu = \dfrac{M_\infty}{M_{tip}} = 0.15$, the freestream Mach number $M_\infty = 0.0975$, and the tip Mach number $M_{tip} = 0.65$.

In the first case study, a medium grid resolution is used for the simulation, with $0.1c_{tip}$ spacing in the finest L1 grids. The gridding system consists of 62 grid zones with a total of approximately 78 million grid points. Figure 5 shows a plot of the PIV plane colored by the vorticity at a delayed azimuth of 5 deg. A color map of a scalar field such as the vorticity is widely used for studying the rotor wake field. Figure 6 gives a plot of the PIV plane colored by the vortex core radius. As shown in this figure, the vortex core radii are computed only at points where the vorticity is above a threshold of 64. It can also be seen that the vortex core radii near Blade 1 (B1) are approximately 55 mm and the core radii around Blades 3 and 4 (B3 and B4) are within the range from 75mm to 175mm. Figure 7 shows a plot of the PIV plane colored by the scaled Q-criterion. Compared to Fig. 5, Fig. 7 provides a more concise representation of the vortex core. Furthermore, instead of guessing the threshold that the vortex core radius is to be computed for grid points where the vorticity is above the threshold value, it is not necessary to guess the threshold when using the scaled Q-criterion. Figure 8 delineates the vortex core radii computed at grid points where the scaled Q-criterion is greater than or equal to 1. In comparison with Fig. 7, Fig. 8 reveals a narrower range of values of the core radius for vortices B1, B3, and B4.

In the second case study, an Adaptive Mesh Refinement (AMR) gridding system is used for the simulation, with 12,239 grid zones and a total of 725 million grid points. Figure 9 shows a plot of the PIV plane colored by the vorticity. Fig. 9 reveals much more flow features than Fig. 5 thanks to grid refinement. Figure 10 shows a plot of the PIV plane colored by the vortex core radius. Vortex core radii are computed at points where the vorticity is above 64. As indicated in the figure, the vortex core radii near Blade 1 (B1) are approximately 50 mm and those around Blades 3 and 4 (B3 and B4) are around 55mm. Figure 11 shows a plot of the PIV plane colored by the scaled Q-criterion. Figure 12 depicts the vortex core radii computed at grid points where the scaled Q-criterion is greater than or equal to 1. Figure 12 reveals a smaller range of values of the core radius for vortices B1, B3, and B4 than Fig. 10.

References

[1]Yamauchi, G., Wadcock, A, Johnson, W., and Ramasamy, M., "Wind Tunnel Measurements of Full-Scale UH-60A Rotor Tip Vortices," AHS 68th Annual Forum, May 2012.

[2]Bhagwat, M.J. and Leishman, J.G., "Correlation of Helicopter Rotor Tip Vortex Measurements," AIAA Journal, Vol. 38, NO. 2, 2000.

[3]Ahmad, J., Yamauchi, G., and Kao, D., "Comparison of Computed and Measured Vortex Evolution for a UH-60A Rotor in Forward Flight," 31st AIAA Applied Aerodynamics Conference, AIAA Paper 2013-3160, June, 2013.

[4]TBD.

[5]Bhagwat, M., and Leishman, J.G., "Correlation of Helicopter Rotor Tip Vortex Measurements," *AIAA Journal,* Vol. 38, NO., 2, 2000, pp. 301-308.

[6]McAlister, K. and Heineck, J., "Measurements of the Early Development of Trailing Vorticity from a Rotor," NASA/TP-2002-211848, AFDD/TR-02-A001, May 2002.

[7]Mula, S.M., Stephenson, J., Tinney, C.E., and Sirohi, J., "Vortex Jitter in Hover," AHS Southwest Region Technical Specialist's Meeting, February 2011.

[8]Ramasamy, M., and Paetzel, R., "Aperiodicity Correlation for Rotor Tip Measurements," AHS 67th Annual Forum, May 2011.

[9]Meakin, R., "Moving Body Overset Grid Methods for Complete Aircraft Tiltrotor Simulations," AIAA Paper 1993-3350, 1993.

[10]Kamkar, S.,J, Wissink, A.M., Sankaran, V., and Jameson, A., "Feature-driven Cartesian Adaptive Mesh Refinement for Vortex-Dominated Flows," Journal of Computational Physics, Vol. 230, No. 16, 2011, pp. 6271-6298.
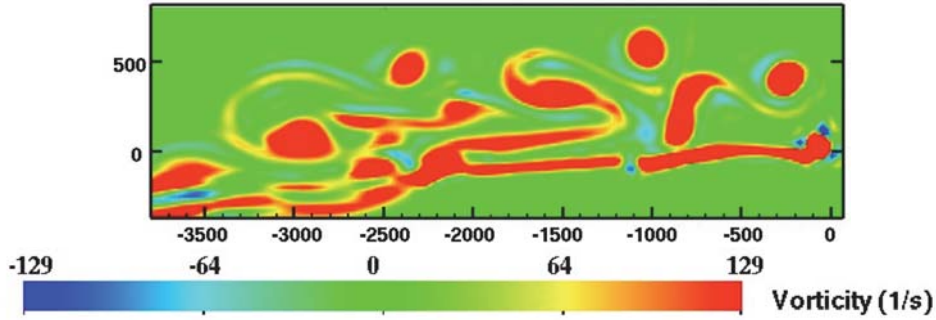
Figure 5. The PIV plane colored by the vorticity at a delayed azimuth of 5 deg, with the flow solution for a UH-60A rotor in forward flight (Run 73, M_{tip} = 0.65, μ = 0.15). The grid system employs a medium grid resolution for the surface mesh, with 0.1Ctip spacing in the L1 grids and a total of 77.5 million points.
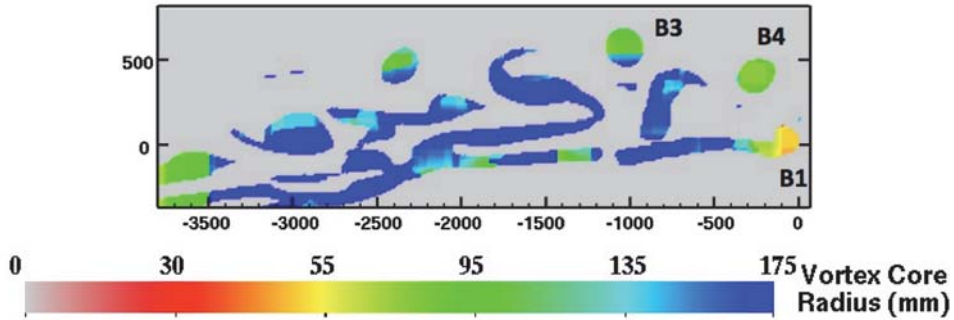

Figure 6. The PIV plane colored by the vortex core radius. Vortex core radii are computed at points where the vorticity is above 64 1/s (see Fig. 5), with the same data set as used for Fig. 5.
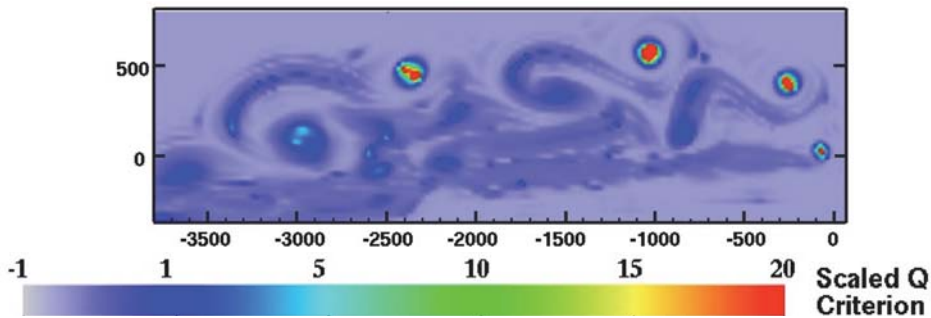
Figure 7. The PIV plane colored by the scaled Q-criterion at a delayed azimuth of 5 deg, with the same data set as used for Fig. 5.
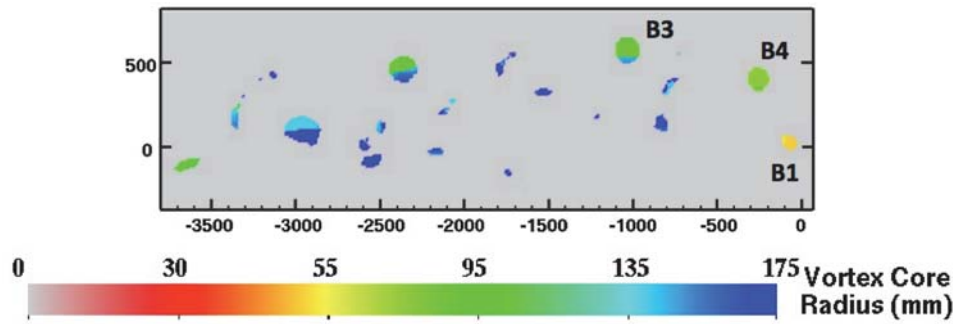
Figure 8. The PIV plane colored by the vortex core radius. Core radii are computed at points where the scaled Q-criterion is great than or equal to 1 (see Fig. 7), with the same data set as used for Fig. 5.
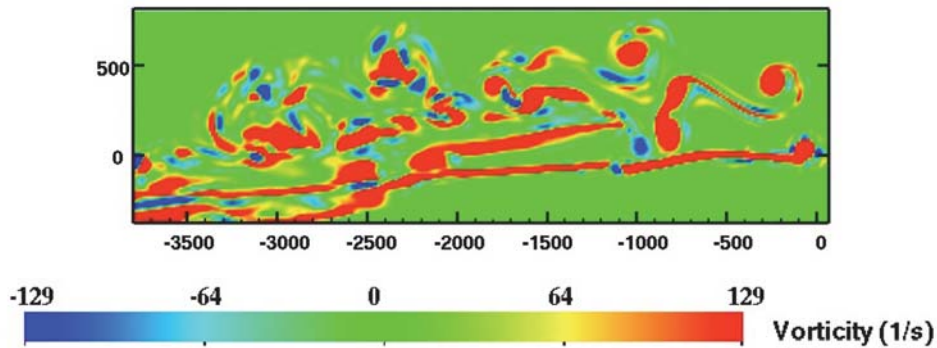

Figure 9. The PIV plane colored by vorticity at a delayed azimuth of 5 deg, with the flow solution for a UH-60A rotor in forward flight (Run 73, M_{tip} = 0.65, μ = 0.15). The grid system uses an Adaptive Mesh Refinement (AMR) grid with 724 million points.
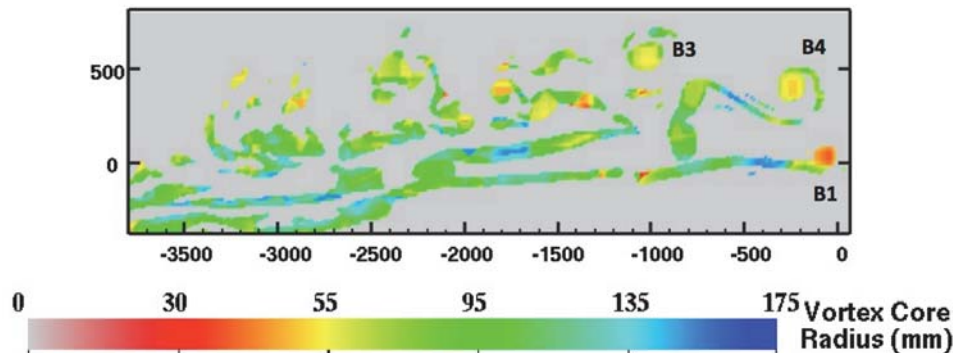

Figure 10. The PIV plane colored by the vortex core radius. Vortex core radii are computed at points where the vorticity is above 64 1/s (see Fig. 9), with the same data set as used for Fig. 9.
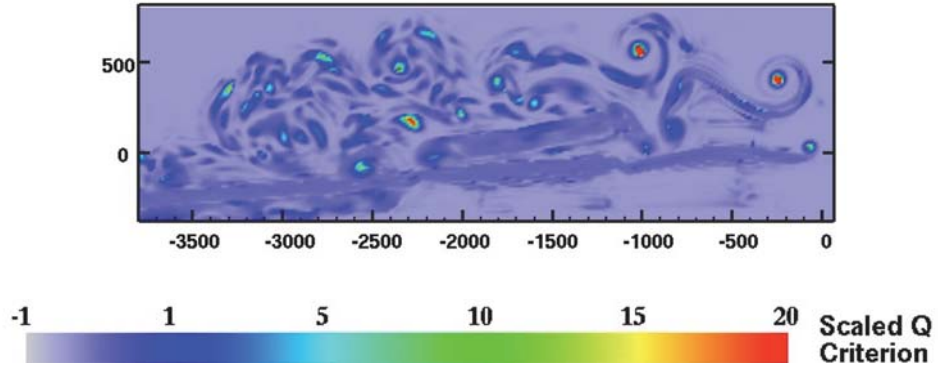
Figure 11. The PIV plane colored by the scaled Q-criterion at a delayed azimuth of 5 deg, with the same data set as used for Fig. 9.
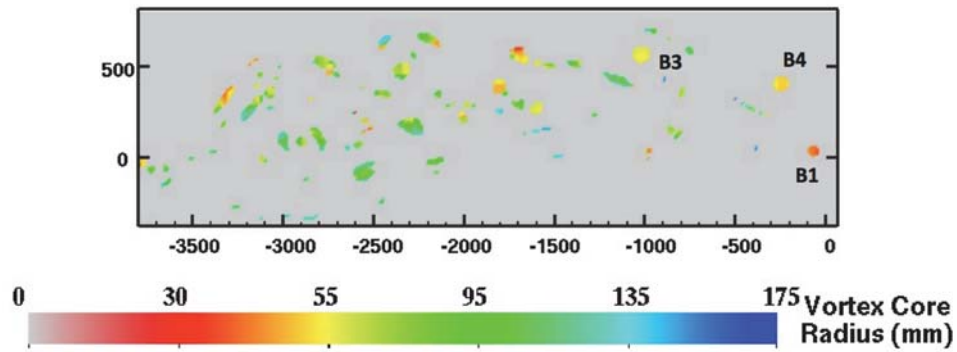

Figure 12. The PIV plane colored by the vortex core radius. Vortex core radii are computed at points where the scaled Q-criterion is great than or equal to 1 (see Fig. 11), with the same data set as used for Fig. 9.

American Institute of Aeronautics and Astronautics